13

Slater–Koster development of Cu–X (X = Cu, O, C, H) parametrization within SCC DFTB method for the improvement of *in silico* quality of the electronic properties studies

© P.A. Kolesnichenko[1], O.E. Glukhova[1,2]

[1] Saratov National Research State University,
410012 Saratov, Russia
[2] First Moscow State Medical University named after I.M. Sechenov,
119991 Moscow, Russia
e-mail: glukhovaoe@info.sgu.ru

Received December 23, 2025
Revised December 23, 2025
Accepted December 23, 2025

A new modification of the Self-Consistent Charge Density Functional Tight Binding (SCC DFTB, sk-files) method has been developed for Cu–X (X = Cu, O, C, H). The electronic part of the sk files was taken as a basis and the repulsive part was improved using „Tango" software package. The following crystal structures were used for a pair of Cu–O atoms with cubic, orthorhombic, and tetragonal syngony, for Cu–C with orthorhombic syngony, for Cu–H with trigonal and hexagonal syngony, and for Cu–Cu with cubic, hexagonal, tetragonal, and monoclinic syngony. The obtained set of Slater–Koster basis functions within SCC DFTB method demonstrates clear advantages over the well-known set ptpb (Periodic Table Baseline Parameter): more accurate reproducibility of the metric parameters of the crystal lattice (lengths of interatomic bonds and translation vectors) — based on comparison with reliable data from experimental studies; consistency of the calculated crystal conductivity with experimental data. Based on the Root Mean Square Deviation (RMSD) for the crystals of Cu–C atomic pair deviation the error of the lattice metric parameters was reduced in 3.9 times, for the pair of atoms Cu–Cu it was reduced in 38 times, and for Cu–H in 36 times, for Cu–O in 6.5 times. Thus, in some cases, it was possible to achieve an improvement of ten times.

Keywords: SCC DFTB, Cu–X (X = Cu, O, C, H), electron transport, Slater–Koster (sk-files) parameters.

DOI: 10.61011/TP.2026.05.63533.345-25

Introduction

Currently, one of the important goals in the electronics and materials science sector is the fabrication of sensor devices to ensure human safety and improve their quality of life. In this regard, a direction is actively developing related to the improvement of devices that detect air quality — gas sensors. One of the most common and promising materials for manufacturing sensitive elements for such devices are thin films — quasi-2*D* structures based on metal oxides [1–4]. Due to a high surface area-to-volume ratio, such structures are a promising material for manufacturing sensors, including sensors for gases, humidity, photodetectors, and biosensors [2,3].

Among the many known metal oxides, copper oxide (Cu_2O) stands out, which belongs to semiconductor materials with *p*-type of conductivity [5]. Copper oxide-based products are non-toxic and relatively low-cost which provides their cost-effectiveness. Such materials are used in photovoltaics and in fabrication of numerous devices, including solar panels, hybrid diodes, biosensors, gas sensors, transistors, lithium-ion batteries and auto-emission cathodes [3,6–12].

Modern advances in computational physics and chemistry are driving the development of digital material science, enabling the prediction of the properties of new materials. One of the most effective methods for modeling atomic and electronic structures is the method of density functional theory (DFT) [12–15], which ensures high accuracy of calculations. However, DFT method is limited because of the stringent requirements to computational resources. As an alternative, semi-empirical methods are increasingly being used, including the Self-Consistent Charge Density Functional Tight Binding (SCC DFTB) method, which combines sufficiently high computational accuracy with high speed of their realization, allowing to study the electronic structure of materials with crystalline supercells containing several thousand atoms, the electronic composition of which includes atoms with such electrons as *s*-, *p*-, *d*- and *f*-electrons [16–18].

In this study, SCC DFTB method was applied using ≪DFTB+≫software [19]. The key tool of the SCC DFTB method includes the Slater–Koster parameters (sk-files, tables), which describe the interaction between atomic orbitals. These tables consist of two parts: the „electronic part", which is responsible for describing the matrix elements of the Hamiltonian, and the repulsive part, which allows modeling the phenomenological nuclear repulsion. Conventional sets of sk-files, e.g., matsci-0-3 [20], do not contain the required parameters to delineate the interaction of Cu–C and Cu–H. This makes the matsci-0-3 set inapplicable for studying systems where copper atoms

interact with C-, H-atoms, which is necessary, for example, when modeling the adsorption of organic analytes on the surface of copper oxide. Therefore, in this study, we used as a basis the existing parameters from ptpb set (Periodic Table Baseline Parameter) [21], which is currently the largest set included in the open database dftb.org [22], describing the interaction of most of the elements of the periodic table, starting from H-atoms to Rn-atoms, and having parameterization sets, including for Cu−C, Cu−H atoms. The electronic part of this parameterization was not considered in this study, since the existing one satisfies the tasks of analyzing and modeling physical adsorption, in which stable covalent bonds do not appear, and the entire interaction of crystal atoms with analytes is delineated by van der Waals forces. The main focus was made on improving the repulsive part, since the existing parameters, as will be shown in this paper, during the search for the minimum total energy of the structure do not ensure the correct structure of the lattice after relaxation making it impossible to analyze the electronic properties of the substance. Thus, the proposed improvement in the repulsive part of Slater−Koster parameters allows for a more accurate description of such systems and to expand the options of SCC DFTB method in sensory tasks.

In this paper, a universal algorithm is proposed for obtaining the repulsive part of sk parameters for SCC DFTB method. The studies of electronic transport were carried out taking into account the Landauer−Butticker formalism using nonequilibrium Green's functions. „Tango“ [23] open source software package was used to improve the parameters and create a new repulsive part.

1. Methods and approaches

1.1. Fundamentals of Slater−Koster method parametrization SCC DFTB

All theoretical studies were carried out using SCC DFTB method, which provides high accuracy in calculating energy and electronic characteristics when using multiatomic supercells [24,25].

The expression for the total energy E_{tot} includes the energy of occupied electron states E_{band}, the energy of interaction of electrons E_{scc} and the energy of repulsion of atomic nuclei E_{rep}. Full energy is described by the following equation (1):

$$E_{tot} = E_{band} + E_{scc} + E_{rep}. \quad (1)$$

Here, E_{band} — is a sum of energies of occupied states. The off-diagonal elements of the Hamiltonian are described using one-center [25] and two-center integrals. The two-center integrals are calculated in advance and are tabulated values, which are used within SCC DFTB method. These values are calculated using the rules of Slater−Koster transform [26,27]. The diagonal elements of the Hamiltonian depend on the effective potential V_{eff}, which is determined by the interaction energy of two different orbitals belonging to different atoms, the electron density, the distance between the atoms, and the polynomial confining potential V_{conf}, which ensures that the electron density is kept in a spherical region near the atom.

The second term in equation (1) E_{scc} — is SCC (Self-Consistent Charge) correction, designed to take into account the change in electron density that occurs due to the interaction of atoms of different chemical elements with each other. This energy depends on redistribution of electron charge density estimated using Mulliken's method, and Coulomb interaction, including exchange-correlation interaction and Hubbard's parameters.

The third term in the equation (1) — E_{rep}, describes the repulsion of two atom nucleii that were omitted in E_{band} and E_{scc}. This interaction is represented as the sum of paired repulsive potentials between atoms i, j:

$$E_{rep} = \sum_{i<j} V_{rep_{i,j}}(r_{i,j}), \quad (2)$$

where the repulsive potential $V_{rep_{i,j}}$ is given by the sum of polynomial functions:

$$V_{rep}(r) = \sum_{p=2}^{6} c_p (r_{cut} - r)^p. \quad (3)$$

This potential should be short-lived and decreasing as the distance between the atoms increases. The cutoff radius r_{cut} is the distance between an atom and its nearest neighbor at which the interatomic interaction energy remains non-zero. The coefficients c_p and degree p define the shape of the spline that determines the properties of the repulsive potential.

1.2. Obtaining the repulsive part of parameterization

„Tango“software package was used to obtain the repulsive part of parametrization of the studied atoms Cu, O, C, H. This is a well-known algorithm that is widely used to solve such problems.

The parameterization algorithm includes six consecutive stages: (1) compilation of a database of DFT calculations; (2) preparation of input data for Tango; (3) setting input parameters for „Tango“; (4) calculation of the repulsive potential; (5) optimization of geometry in SCC DFTB; (6) comparison with the reference DFT structure. The process continues iteratively from the third step until an error of less than 5 % is achieved.

Let's consider this scheme sequentially, step by step.

1. The database was compiled at the first stage. For the studied structures its compilation included sequential registration of geometric and energy parameters after a single-point DFT calculation with a step-by-step change in the initial geometry (compression, stretching, twisting and detachment of the atom).

2. Input data for Tango: type, electron shell configuration, maximum angular momentum, database used.

3. The third step includes specifying the values for the minimum ($r_{\min}$) and maximum (r_{cut}) distances between atoms at which the repulsive potential is determined.

4. The next step is to calculate the repulsive potential in Tango program. The calculated potentials are written into initial sk-files taken from ptpb set where the electronic part is contained.

Then the atomic lattices of the studied structures are optimized using the repulsion potentials of atomic pairs (and the entire set as a whole) obtained in the previous step using SCC DFTB method.

6. At the last stage, the optimized structure using SCC DFTB method from the previous step is compared with the reference structure improved using DFT method. The following quantities are compared: the lengths of the structures' translation vectors and the bond lengths of the atoms in them. The error is calculated as a percentage for each value, after which the total error for this structure is calculated.

If the value of the obtained error is below the specified value of 5%, then the calculation is complete. Otherwise — return to step 3 with other parameters. In this way, it was possible to obtain repulsive potentials that correctly describe the relaxation of the lattice geometry parameters in the studied structures.

To find the repulsion potential of Cu−O, Cu−Cu, Cu−C, Cu−H the equillibrium supercells from the database next-gen.materialsproject. org [28] were applied with various types of crystalline lattices. The supercells were isotropically scaled over the volume range from 99% to 131% in 1% increments to compile a database with different values of the total energy and forces acting on each atom. One-point analysis of full energy was made for each case using DFT in GPAW software [29] with ASE library [30] and GGA-PBE functional, in the planar wave approximation. The Brillouin zone partitioning by the Monkhorst−Pack method was performed with a 16x16x16 grid for cubic cells, triclinic and orthorhombic cells, and 32x16x16 for hexagonal ones. Similarly, a database with energy calculations using SCC DFTB method was obtained with the same Monkhorst−Pack grid.

2. Results and discussion

2.1. Research object

The main object of the study is copper oxide I having a cubic crystal lattice due to its pronounced semiconductor properties and wideband gap (about 2.17 eV [31,32]), which is promising in respect of using this material as a detecting element in gas sensors. In addition, Cu_2O crystal is low-energy, hence it is stable. The equilibrium unit cell of the crystal was taken from the open database next-gen.materialsproject.org with the identification number mp-361 [33]. From here on, for clarity, the considered cells will be designated by numbers from the database.

To compile the database of „Tango“ program, various supercells of materials were used, in which there was pure copper, or it was bound to atoms necessary for the set of parametrizations, namely C, O, H. Among them, the following were selected for Cu−O: mp-361 with a cubic lattice and symmetry group $Pn\bar{3}m1$; mp-760432 [34] with an orthorhombic lattice and symmetry group Fdd2; mp-1478 [35] with a tetragonal lattice and symmetry group $I\bar{4}/amd$; and mp-1692 [36] also with a tetragonal lattice and symmetry group $P\bar{4}/mmc$. For Cu−C, the only unit cell mp-1213653 [37] with an orthorhombic lattice and symmetry group Cmmm available in the open database was chosen. For Cu−H, two cells from the database were selected: mp-1225705 [38] with a trigonal crystal lattice and symmetry group $P\bar{3}m1$, and mp-24093 [39] with a hexagonal lattice and symmetry group $P\bar{6}mc$. For pure copper, four unit cells were chosen: mp-30 [40] with a cubic lattice and symmetry group $Fm\bar{3}m$, mp-989695 [41] with a hexagonal lattice and symmetry group $P\bar{6}/mmc$, mp-1010136 [42] with a tetragonal lattice and symmetry group I4/mmm, and mp-1059259 [43] with a monoclinic lattice and symmetry group P12/m1.

To compile the database and subsequently compare the obtained results, predominantly stable, equilibrium cells were selected where they were available in the open database; otherwise, the only available cells or the only available cells of a given syngony were selected. Moreover, sk-parameters, which were not considered here, but were required for SCC DFTB analysis (e.g., C−C, O−O, H−H and etc.) were taken directly from the ptpb set without any changes.

2.2. Comparison of geometry

The geometric parameters were compared between DFT optimization, which was taken as a reference, and SCC DFTB optimization with ptpb parameters and improved parameters obtained in this study. The root-mean-square deviation (RMSD) metric was used to quantify the differences. The calculation was made providing for the optimal spatial superposition of structures, which made it possible to exclude the effect of global shift and rotation and evaluate only the internal changes in the position of atoms. Optimal superposition was performed using Kabsch algorithm [44].

Let $\mathbf{P} = \{\mathbf{p}_1, \ldots, \mathbf{p}_N\}$ and $\mathbf{Q} = \{\mathbf{q}_1, \ldots, \mathbf{q}_N\}$ — are the sets of Cartesian coordinates of the atoms of reference ($\mathbf{p}_1 = (x_1, y_1, z_1)$ and etc.) and improved ($\mathbf{q}_1 = (x_1, y_1, z_1)$ and etc.) structures, respectively. At the first stage, both structures are centered relative to their geometric centers according to formulas (4) and (5):

$$\overline{\mathbf{p}} = \frac{1}{N}\sum_{i=1}^{N}\mathbf{p}_i, \quad \overline{\mathbf{q}} = \frac{1}{N}\sum_{i=1}^{N}\mathbf{q}_i, \tag{4}$$

$$\mathbf{P}_c = \mathbf{P} - \overline{\mathbf{p}}, \quad \mathbf{Q}_c = \mathbf{Q} - \overline{\mathbf{q}}, \tag{5}$$

where N — total number of the atoms in structure.

Next, a covariance matrix is constructed that describes the correlation between the coordinates of atoms in two

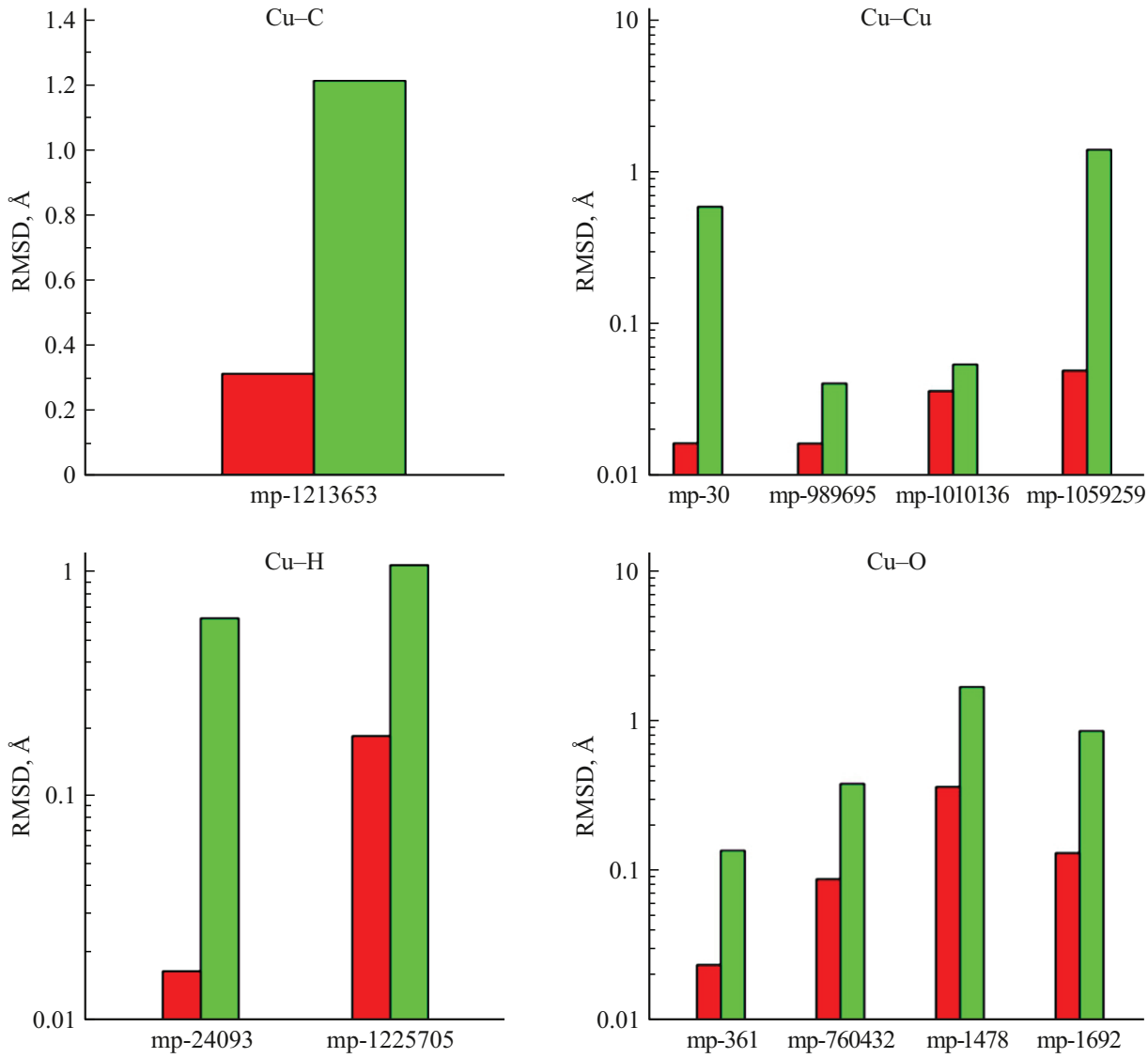

Figure 1. RMSD for parameters obtained in this study and ptpb set parameters, compared.

structures after centering, using the formula (6):

$$\mathbf{C} = \mathbf{P}_c^{\bullet}\,\mathbf{Q}_{c\bullet}, \tag{6}$$

where $\mathbf{P}_c^{\bullet}$ — is a transposed matrix.

To find the optimal rotation, the singular value decomposition (SVD) of the matrix is applied according to formula (7). It allows to efficiently find a rotation that maximizes the match between structures:

$$\mathbf{C} = \mathbf{V}\mathbf{\Sigma}\mathbf{W}^{\bullet}, \tag{7}$$

where $\mathbf{V}, \mathbf{W} \in R^{3\times 3}$ — are orthogonal matrices (whose columns are called left and right singular vectors), $\mathbf{\Sigma}$ — is a diagonal matrix with non-negative singular values on the diagonal.

From SVD the matrix of optimal rotation $\mathbf{R}$ is found by the formula (8):

$$\mathbf{R} = \mathbf{V}\mathbf{W}^{\bullet}. \tag{8}$$

Applying the obtained rotation matrix to the centered reference structure, we obtain aligned coordinates (9):

$$\mathbf{P}_{\text{aligned}} = \mathbf{P}_c\mathbf{R}. \tag{9}$$

After alignment of the structures coordinates, the quantitative indicator of the difference in geometry (RMSD) was calculated directly using formula (10):

$$\text{RMSD} = \sqrt{\frac{1}{N}\sum_{i=1}^{N} \|\mathbf{P}_{\text{aligned},i} - \mathbf{Q}_{c,i}\|^2}, \tag{10}$$

where the operator $\|\cdot\|$ — is the Euclidean norm (length) of the three-dimensional vector of the difference in coordinates of the i-th atom after superposition of the structures.

Next, the RMSD for all the studied supercells in the summary table will be considered. After which, in Fig. 1, these indicators will be graphically reflected. Then,

RMSD summary table for all the studied supercells

Pair of atoms	Cell	Syngony — symmetry group	$RMSD_{work}$, Å	$RMSD_{ptpb}$, Å
Cu−C	mp-1213653	Orthorombic — Cmmm	0.310525	1.209862
Cu−Cu	mp-30	Cubic — $Fm\bar{3}m$	0.009198	0.030557
	mp-989695	Hexagonal — P6/mmc	0.002959	0.040270
	mp-1010136	Tetragonal — I4/mmm	0.035908	0.053578
	mp-1059259	Monoclinic — P12/m1	0.048898	1.373024
Cu−H	mp-24093	Hexagonal — P6mc	0.016337	0.579823
	mp-1225705	Trigonal — $P\bar{3}m1$	0.176155	0.992251
Cu−O	mp-361	Cubic — $Pn\bar{3}m1$	0.023443	0.135143
	mp-760432	Orthorhombic — Fdd2	0.087286	0.375996
	mp-1478	Tetragonal — I4/amd	0.358350	1.660172
	mp-1692	Tetragonal — P4/mmc	0.130236	0.844074

qualitative comparisons of the crystal structures in the figures will be given when superimposing the appropriate models before and after optimization by various methods for the considered pairs of atoms.

As can be seen from the table, the parameters found in this study have RMSD values (relative to the structure relaxed by DFT method) that do not exceed 1 Å, while the ptpb set gives RMSD that is several times larger in all the cases considered. Thus, the authors of the study managed to achieve a tenfold improvement of the result of searching for a geometric configuration with minimal energy. Fig. 1 illustrates the comparison of RMSD in graphic view. The RMSD values obtained in the work are shown in red, the ptpb set values are shown in green. It should be noted that for Cu−C atoms the RMSD is given on a linear graph, since the structure is unique. In other cases, for clarity, the RMSD value is shown on a logarithmic scale.

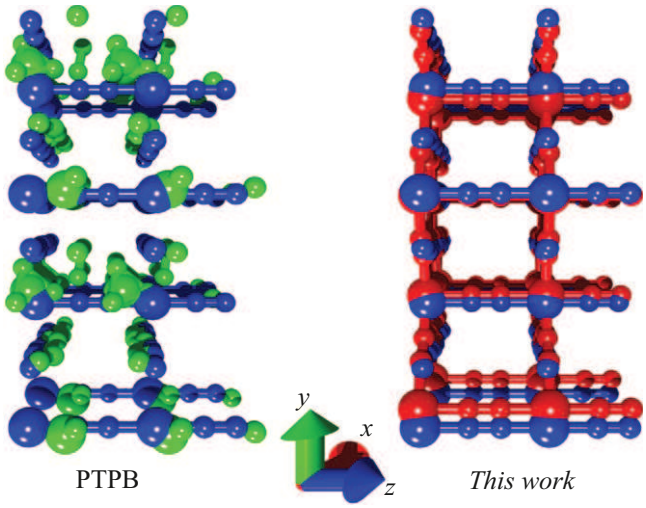

Figure 2. The crystalline lattices of mp-1213653 cell, compared.

Analysis of parameters for the pair of Cu−C atoms

Fig. 2 illustrates the comparison of crystalline structures of Cu−C. Here and below, the positions of atoms obtained as a result of DFT optimization are shown in blue; they are taken as a standard. The positions of atoms after optimization of geometry via SCC DFTB method with the ptpb parameter set are shown in green, and those with the parameter set improved in this work are shown in red.

From Fig. 2 it can be seen that the ptpb parametrization in this case, when searching for the minimum energy, „destroys“ the crystal structure, all bonds between Cu and C atoms are broken, and all periodicity is lost. At the same time, the improvements proposed in this study show, on average, the correct representation of lattice, while maintaining bond lengths and translational symmetry of the crystal, slightly differing in the positions of carbon atoms (they are shown in a smaller size). Thus, reducing the error relative to DFT method allows obtaining a physically correct structure that can be used in further calculations.

Analysis of parameters for the pair of atoms Cu−Cu

Next, the parameters of the interaction of atoms of one chemical element were investigated. Figure 3 shows a comparison of the atomic positions for different supercell pairs of Cu−Cu atoms studied in this paper.

In Fig. 3, *a* it can be seen that in this case, for crystalline copper, the improved parameters give a result almost indistinguishable from DFT (almost no red color), while the ptpb parameters show an optimization result different from DFT for all atoms in the crystal. We can identify the structure in Fig. 3, *d* for it, the ptpb set after optimizing

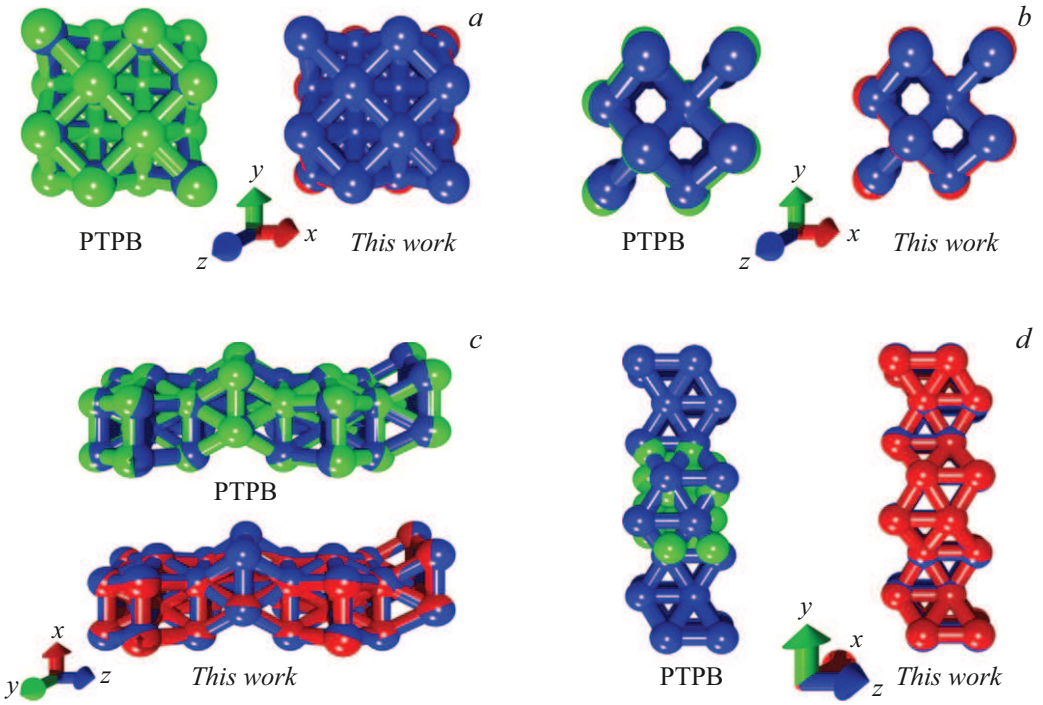

Figure 3. Crystalline lattices of the cells of Cu−Cu, compared. Different structures are denoted by the letters: *a* — mp-30, *b* — mp-1010136, *c* — mp-989695, *d* — mp-1059259.

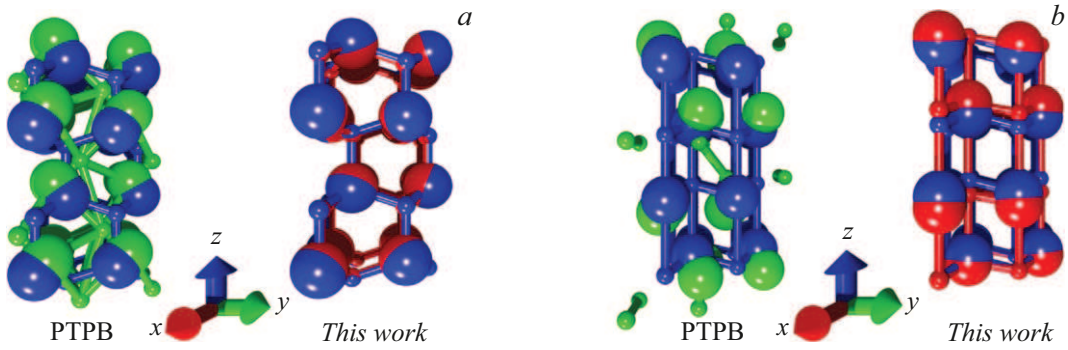

Figure 4. Crystalline lattices of the cells of Cu−H, compared. Different structures are denoted by the letters: *a* — mp-24093, *b* — mp-1225705

the metric parameters of the cell, groups all copper atoms to each other, and the bond lengths become smaller than the effective radius of the copper atom. Thus, after SCC DFTB optimization of this supercell, the periodicity in the crystal is lost. The parameters obtained in this paper, on the contrary, preserve the crystalline structure of the substance.

Analysis of parameters for the pair of atoms Cu−H

Figure 4 shows a comparison of the atomic positions for different supercell pairs of Cu−H atoms studied in this paper.

In Fig. 4, it can be seen that, as in the case of mp-1213653 and mp-1059259 cells, the ptpb set does not represent the crystalline structure of the substance; the bond lengths of the atoms in the crystal are distorted, and their position is disrupted. Moreover, the improved set, as in all previous cases, correctly reflects the metric parameters of the cell and closely matches the reference DFT cell.

Analysis of parameters for the pair of atoms Cu−O

Figure 5 shows a comparison of the atomic positions for different supercell pairs of Cu−O atoms outlined herein.

In Fig. 5, *c* it is evident that as a result of optimization by ptpb parameters the unit cell was destroyed, the atoms were carried to large distances, and therefore the obtained results are completely physically incorrect and erroneous. At the same time, the parameters in this work, as for other supercells, show fairly correct results, due to which the

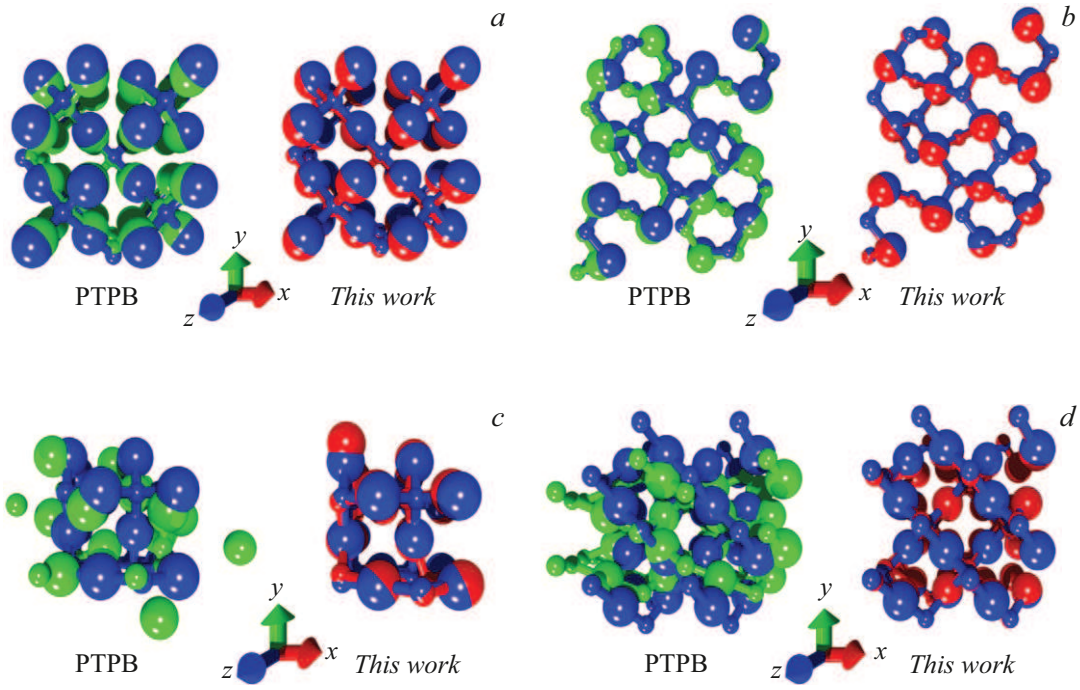

Figure 5. Crystalline lattices of the cells of Cu−O, compared. Different structures are denoted by the letters: *a* — mp-361, *b* — mp-760432, *c* — mp-1478, *d* — mp-1692

obtained cells can be used for further research. In Fig. 5, *d*, just as in the previous case, the ptpb parameters did not cope with the task of finding the minimum energy during the change of atomic positions in the crystal lattice.

2.3. Electronic transport

Using the new improved parameters for copper oxide, transport analysis was made using SCC DFTB method and this allowed to calculate the conductivity (resistance) of the structure. Cu_2O mp-361 cell with a cubic lattice was chosen as the object of study due to its experimentally established electronic properties, a wide band gap equal to about 2.17 eV [31,32], and also due to the minimal error in the cell metric parameters after SCC DFTB analysis compared to DFT approach.

In the first step, the density of states (DOS) for the given structure was calculated, shown in Fig. 6 on the left, followed by transmittance function T, shown in Fig. 6 on the right. Red color denotes the Fermi level of −1.4036 eV.

From the density of states graph in Fig. 6, one can see that the band gap is about 2 eV. The calculated value differs from the experimental one by 7.83 %. The calculated result proves correctness and accuracy of the parameters obtained in this work, as well as the correspondence of the results found by SCC DFTB method with the experimental data. It is also evident from the graph of the transmittance function that there are approximately 0.6 conduction channels at the Fermi level. Using the Landauer−Buttiker formalism and the nonequilibrium Green's function method, the calculated conductivity makes $2.044 \cdot 10^{-9}$ S, which is equal to $4.891 \cdot 10^{8}\ \Omega$. This resistance is in complete agreement with the experimentally determined value, equal to the order of $10^{8}\ \Omega$ for low temperatures ($< 100\,^{\circ}$C) [45–47], which also confirms the correctness of the obtained parameters for the structures' conductivity.

Conclusion

The study provides and implements a brand-new modification of SCC-DFTB method parametrization for Cu−X (X = Cu, O, C, H) interactions based on the improvement of the repulsion part of Slater−Koster parameters (sk-files) while preserving the electron part from the relevant ptpb set [21]. This kind of modification is essential because, despite the widespread use of semi-empirical methods in materials science, their applicability to systems with transition metals, e.g., copper, is often limited in view of insufficient accuracy in reproducing the geometry and electronic properties. In particular, as shown in the study, the original parameters of ptpb lead to significant distortions of the lattice during relaxation, up to the complete destruction of periodicity and unphysical compression of interatomic distances, which makes further analysis of the electronic structure and transport properties impossible.

The proposed approach, based on the use of „Tango“ [23] software for constructing improved repulsive potentials, has made it possible to achieve significant progress in the modeling accuracy. Using eleven supercells covering different crystallographic syngonies (cubic, tetragonal, orthorhombic, hexagonal and monoclinic) as an example, it was demon-

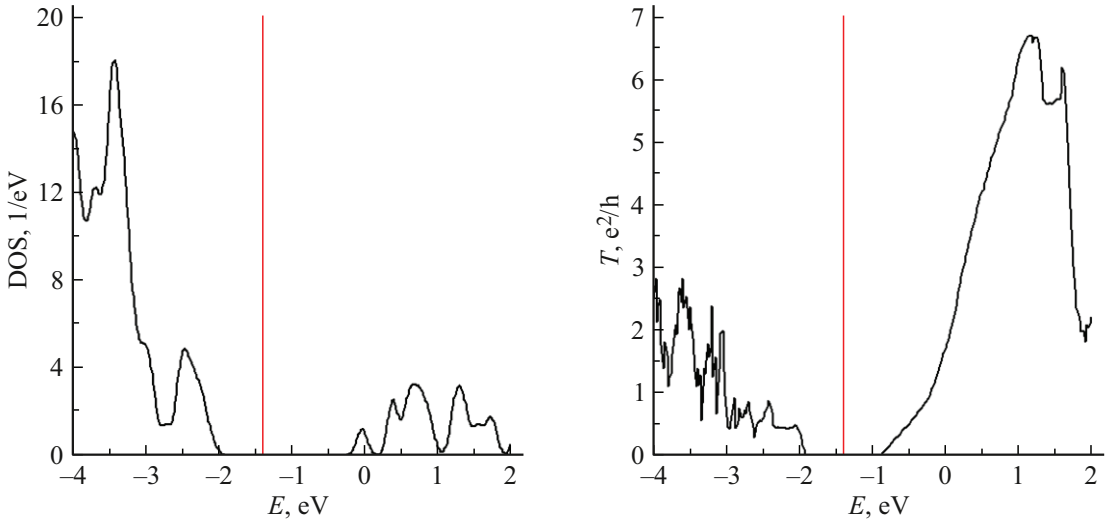

Figure 6. DOS graph (on the left) and transmission function (on the right) for Cu_2O.

strated that the modified parameters reduce the error in reproducing interatomic distances and translation vectors relative to the reference DFT calculations in 5−38 times, depending on the system, compared to the original ptpb set. For crystals of a pair of Cu−C atoms, the error in the metric lattice parameters was reduced by 3.9 times, for a pair of Cu−Cu atoms by 38 times, for a pair of Cu−H atoms by 36 times, for Cu−O by 6.5 times, as shown by RMSD analysis. Thus, in some cases it was possible to achieve an improvement of tens of times, which provided new options in modeling the analytes' adsorption on the surface of copper oxides - a problem that had not previously been solved using standard sets of parameters, such as matsci-0-3 [20].

Improving the accuracy of geometric parameters directly affected the reliability of the electronic properties prediction. Using Cu−O (mp-361) crystal as an example, the electron density of states (DOS) and the transmittance function were calculated using Landauer−Buttiker formalism within the framework of nonequilibrium Green's functions. The obtained band gap (~ 2.0 eV) differs from the experimental value (~ 2.17 eV) [31,32] by only 7.8%, which is a high accuracy for a semi-empirical method and confirms the correctness of the proposed parameterization. Moreover, the calculated electrical resistance of the structure ($4.891 \cdot 10^8\ \Omega$) differs from the experimental data for thin Cu−O films at temperatures below 100 °C by no more than 10% [45–47]. This indicates that the modified parameters not only accurately describe the geometry, but also adequately outline the physics of electron transport a key aspect for applications in sensors and microelectronics.

It should be emphasized that accurate modeling of electronic properties of copper oxides is critical for the development of chemoresistive gas sensors, where Cu−O acts as a sensitive detecting element [1,5]. Existing DFT calculations of such systems are limited by the supercell size and computational costs, while SCC-DFTB method allows studying adsorption, diffusion, and charge transfer processes on nanoscale models with thousands of atoms [16–18].

Thus, the developed Slater−Koster parameters not only provide high accuracy of modeling the geometric and electronic properties of copper-based crystals, but also open up new possibilities for *in silico* design of functional materials. They enable reliable modeling of adsorption and electron transport processes in complex nanostructures, which is especially pivotal for the development of chemoresistive gas sensors based on Cu−O. The proposed approach to adjusting the repulsive part of the parameters can be extended to other transition metal systems, contributing to the creation of more universal and reliable databases for SCC-DFTB.

Conflict of interest

The authors declare that they have no conflict of interest.

References

[1] S. Steinhauer. Chemosensors, **9**, 51 (2021). DOI: 10.3390/chemosensors9030051
[2] D. Nunes, A. Pimentel, A. Gonçalves, S. Pereira, R. Branquinho, P. Barquinha, E. Fortunato, R. Martins. Semicond. Sci. Technol., **34**, 043001 (2019). DOI: 10.1088/1361-6641/ab011e
[3] Z. Zhang, S. Zhang, S. Liu, M. Wang, G. Fu, L. He, Y. Yang, S. Fang. Sens. Actuators B Chem., **220**, 84 (2015). DOI: 10.1016/j.snb.2015.05.089
[4] P.T. Moseley. Meas. Sci. Technol., **28**, 082001 (2017). DOI: 10.1088/1361-6501/aa7443
[5] H.J. Kim, J.H. Lee. Sens. Actuators B Chem., **192**, 607 (2014). DOI: 10.1016/j.snb.2013.11.005
[6] A.S. Zoolfakar, R.A. Rani, A.J. Morfa, A.P. O'Mullane, K. Kalantar-zadeh. J. Mater. Chem. C, **2**, 5247 (2014). DOI: 10.1039/C4TC00345D

[7] Q. Zhang, K. Zhang, D. Xu, G. Yang, H. Huang, F. Nie, C. Liu, S. Yang. Prog. Mater. Sci., **60**, 208 (2024). DOI: 10.1016/j.pmatsci.2013.09.003
[8] J.J.M. Vequizo, C. Zhang, M. Ichimura. Thin Solid Films, **597**, 83 (2015). DOI: 10.1016/j.tsf.2015.11.034
[9] M. Izaki, T. Saito, T. Ohata, K. Murata, B.M. Fariza, J. Sasano, T. Shinagawa, S. Watase. ACS Appl. Mater Interfaces, **4**, 3558 (2012). DOI: 10.1021/am3006093
[10] C.-L. Hsu, J.-Y. Tsai, T.-J. Hsueh. Sens. Actuators B Chem., **224**, 95 (2016). DOI: 10.1016/j.snb.2015.10.018
[11] H.A. Al-Jawhari. Mater. Sci. Semicond. Process., **40**, 241 (2015). DOI: 10.1016/j.mssp.2015.06.063
[12] M. Valvo, D. Rehnlund, U. Lafont, M. Hahlin, K. Edström, L. Nyholm. J. Mater. Chem. A, **2**, 9574 (2014). DOI: 10.1039/C4TA01361A
[13] G. Kresse, D. Joubert. Phys. Rev. B, **59**, 1758 (1999). DOI: 10.1103/PhysRevB.59.1758
[14] P. Giannozzi, O. Andreussi, T. Brumme, O. Bunau, M. Buongiorno Nardelli, M. Calandra, R. Car, C. Cavazzoni, D. Ceresoli, M. Cococcioni, N. Colonna, I. Carnimeo, A. Dal Corso, S. de Gironcoli, P. Delugas, R.A. DiStasio Jr, A. Ferretti, A. Floris, G. Fratesi, G. Fugallo, R. Gebauer, U. Gerstmann, F. Giustino, T. Gorni, J. Jia, M. Kawamura, H.-Y. Ko, A. Kokalj, E. Küçükbenli, M. Lazzeri, M. Marsili, N. Marzari, F. Mauri, N.L. Nguyen, H.-V. Nguyen, A. Otero-de-la-Roza, L. Paulatto, S. Poncé, D. Rocca, R. Sabatini, B. Santra, M. Schlipf, A.P. Seitsonen, A. Smogunov, I. Timrov, T. Thonhauser, P. Umari, N. Vast, X. Wu, S. Baroni. J. Phys.: Condens. Matter, **29**, 465901 (2017). DOI: 10.1088/1361-648X/aa8f79
[15] J.M. Soler, E. Artacho, J.D. Gale, A. García, J. Junquera, P. Ordejón, D. Sánchez-Portal. J. Phys.: Condens. Matter, **14**, 2845 (2002). DOI: 10.1088/0953-8984/14/11/302
[16] S.J. Clark, M.D. Segall, C.J. Pickard, P.J. Hasnip, M.J. Probert, K. Refson, M.C. Payne. Z. Kristallogr., **220**, 567 (2005). DOI: 10.1524/zkri.220.5.567.65075
[17] H. Liu, G. Seifert, C. Di Valentin. J. Chem. Phys., **150**, 094703 (2019). DOI: 10.1063/1.5085190
[18] G. Zheng, S. Irle, K. Morokuma. Chem. Phys. Lett., **412** (1–3), 210 (2005). DOI: 10.1016/j.cplett.2005.06.105
[19] S. Manzhos. Chem. Phys. Lett., **643**, 16 (2016). DOI: 10.1016/j.cplett.2015.11.007
[20] B. Hourahine, B. Aradi, V. Blum, F. Bonafé, A. Buccheri, C. Camacho, C. Cevallos, M.Y. Deshaye, T. Dumitrică, A. Dominguez, S. Ehlert, M. Elstner, T. van der Heide, J. Hermann, S. Irle, J.J. Kranz, C. Köhler, T. Kowalczyk, T. Kubař, I.S. Lee, V. Lutsker, R.J. Maurer, S.K. Min, I. Mitchell, C. Negre, T.A. Niehaus, AM. N. Niklasson, A.J. Page, A. Pecchia, G. Penazzi, M.P. Persson, J. Řezáč, C.G. Sánchez, M. Sternberg, M. Stöhr, F. Stuckenberg, A. Tkatchenko, V.W. Yu, T. Frauenheim. J. Chem. Phys., **152**, 124101 (2020). DOI: 10.1063/1.5143190
[21] M. Cui, K. Reuter, J.T. Margraf. J. Chem. Theory Comput., **20**, 5276 (2014). DOI: 10.1021/acs.jctc.4c00228
[22] DFTB. Available at: https://dftb.org/parameters/ (access date: 14-07-2025)
[23] M. Van den Bossche, H. Grönbeck, B. Hammer. J. Chem. Theory Comput., **14**, 2797 (2018). DOI: 10.1021/acs.jctc.8b00039
[24] P. Koskinen, V. Makinen. Comput. Mater. Sci., **47**, 237 (2009). DOI: 10.48550/arXiv.0910.5861
[25] M. Wahiduzzaman, A.F. Oliveira, P. Philipsen, L. Zhechkov, E. van Lenthe, H.A. Witek, T. Heine. J. Chem. Theory Comp., **9** (9), 4006 (2013). DOI: 10.1021/ct4004959
[26] T. Frauenheim, G. Seifert, M. Elstner, Z. Hajnal, G. Jungnickel, D. Porezag, S. Suhai, R. Scholz. Phys. Status Solidi B, **217**, 41 (2000). DOI: 10.1002/(SICI)1521-3951(200001)217:1¡41::AID-PSSB41¿3.0.CO;2-V
[27] J.C. Slater, G.F. Koster. Phys. Rev., **94**, 1498 (1954). DOI: 10.1103/PhysRev.94.1498
[28] A. Jain, S.P. Ong, G. Hautier, W. Chen, W.D. Richards, S. Dacek, S. Cholia, D. Gunter, D. Skinner, G. Ceder, K.A. Persson. APL Mater., **1**, 011002 (2013). DOI: 10.1063/1.4812323
[29] M.K. Kjeldsen, J. Enkovaara, C. Rostgaard, J. Olsen, K.S. Thygesen. Phys. Rev. B, **74**, 235102 (2006). DOI: 10.1103/PhysRevB.74.235102
[30] A.H. Larsen, J.J. Mortensen, J. Blomqvist, I.E. Castelli, R. Christensen, M. Dułak, J. Friis, M.N. Groves, B. Hammer, C. Hargus, E.D. Hermes, P.C. Jennings, P.B. Jensen, J. Kermode, J.R. Kitchin, E.L. Kolsbjerg, J. Kubal, K. Kaasbjerg, S. Lysgaard, J.B. Maronsson, T. Maxson, T. Olsen, L. Pastewaka, A. Peterson, C. Rostgaard, J. Schiøtz, O. Schütt, M. Strange, K.S. Thygesen, T. Vegge, L. Vilhelmsen, M. Walter, Z. Zeng, K.W. Jacobsen. J. Phys.: Condens. Matter, **29**, 273002 (2017). DOI: 10.1088/1361-648X/aa680e
[31] C.G. Ribbing, A. Roos. *Copper oxides (Cu–O, CuO)*. In: *Handbook of Optical Constants of Solids* (1998), p. 875–882. DOI: 10.1016/B978-0-08-055630-7.50054-7
[32] L.-P. Mei, J.-J. Feng, L. Wu, J.-R. Chen, L. Shen, Y. Xie, A.-J. Wang. Microchim. Acta, **183**, 2039 (2016). DOI: 10.1007/s00604-016-1845-0
[33] Data for Cu–O (Materials Project ID: mp-361), database version v2025.06.09. Materials Project. 2025. DOI: 10.17188/1207131
[34] Data for Cu–O (Materials Project ID: mp-760432), database version v2025.06.09. Materials Project. 2025. DOI: 10.17188/1291638
[35] Data for Cu–O (Materials Project ID: mp-1478), database version v2025.06.09. Materials Project. 2025. DOI: 10.17188/1190887
[36] Data for CuO (Materials Project ID: mp-1692), database version v2025.06.09. Materials Project. 2025. DOI: 10.17188/1192239
[37] Data for CuC (Materials Project ID: mp-1213653), database version v2025.06.09. Materials Project. Available at: https://next-gen.materialsproject.org/materials/mp-1213653?chemsys=Cu-C (Access date: 16-09-2025).
[38] Data for CuH (Materials Project ID: mp-1225705), database version v2025.06.09. Materials Project. Available at: https://next-gen.materialsproject.org/materials/mp-1225705?chemsys=Cu-H (Access date: 16-09-2025).
[39] Data for CuH (Materials Project ID: mp-24093), database version v2025.06.09. Materials Project. DOI: 10.17188/1199906
[40] Data for Cu (Materials Project ID: mp-30), database version v2025.06.09. Materials Project. DOI: 10.17188/1204433
[41] Data for Cu (Materials Project ID: mp-989695), database version v2025.06.09. Materials Project. DOI: 10.17188/1282187
[42] Data for Cu (Materials Project ID: mp-1010136), database version v2025.06.09. Materials Project. DOI: 10.17188/1326840

[43] Data for Cu (Materials Project ID: mp-1059259), database version v2025.06.09. Materials Project. Available at: https://next-gen.materialsproject.org/materials/mp-1059259?formula=Cu (Access date: 16-09-2025).
[44] W. Kabsch. Acta Crystallographica Section A, **34** (6), 827 (1978). DOI: 10.1107/S0567739478001680
[45] R. Padyath, J. Seth, S.V. Babu. Thin Solid Films, **239**, 8 (1994). DOI: 10.1016/0040-6090(94)90101-5
[46] F.M. Li, R. Waddingham, W.I. Milne, A.J. Flewitt, S. Speakman, J. Dutson, M. Thwaites. Thin Solid Films, **520**, 1278 (2011). DOI: 10.1016/j.tsf.2011.04.192
[47] A. Ogwu, T. Darma, E. Bouquerel. J. Achiev. Mater. Manuf. Eng., **24**, 121 (2007).

Translated by T.Zorina